Higgs portal vector dark matter interpretation: review of Effective Field Theory approach and ultraviolet complete models

Mohamed Zaazoua [1], Loan Truong [2], Kétévi A. Assamagan [3], Farida Fassi [1]

[1] *Mohammed V University in Rabat, Faculty of Science*
[2] *University of Johannesburg, Department of Mechanical Engineering Science*
[3] *Brookhaven National Laboratory (BNL)*

March 22, 2022

A review of the Higgs portal-vector dark matter interpretation of the spin-independent dark-matter nucleon elastic scattering cross section is presented, where the invisible Higgs decay width measured at the LHC is used. Effective Field Theory and ultraviolet complete models are discussed. LHC interpretations show only the scalar and Majorana dark-matter scenarios; we propose to include interpretation for vector dark matter in the EFT and UV completions theoretical framework. In addition, our studies suggest an extension of the LHC dark matter interpretations to the sub-GeV regime.

1 Introduction

The existence of a Dark Matter (DM) component of the universe is now firmly established, supported by astrophysical observations [1]. While the nature of the DM particles and their interactions remain an open question, viable candidates must lie in theories beyond the Standard Model (BSM). A particularly interesting class of candidates are weakly interacting massive particles (WIMP). They appear in many BSM theories. Due to their weak-scale interaction cross-section, they can accurately reproduce the observed DM abundance in the Universe today[2].

At the LHC, experiments have explored Higgs portal scenarios in which the 125 GeV Higgs boson has substantial coupling with WIMP candidates (such as singlet scalar S, vector V, fermion χ) to induce interaction between WIMP and nucleon; the WIMP could be invisible decay products of the Higgs boson [3–16]. Therefore, limits on the branching ratio ($\mathcal{B}_{H\to\text{inv}}$) from invisible Higgs decay can be used to set upper bounds on spin-independent DM-nucleon scattering cross section σ^{SI}(WIMP-N). LHC interpretations complement direct and indirect detection results. [17–22].

The Effective Field Theory (EFT) approach is based on a decription of unkown DM-Standard Model (SM) interactions in a very economical way. This has attracted significant attention, especially because of its simplicity and flexibility which allows it to be used in vastly different search contexts. For the scalar and Majorana fermion WIMP candidates, the EFT approach [7, 8] can be safely used. Hence, the EFT approach [7] is used in LHC Run–1 papers [23, 24]. Unfortunately, the validity of this approach for the vector-DM case has been questioned and its limitations recognized by the theoretical and experimental communities [25]. Recent efforts to develop more model-independent approaches to DM searches stimulated this study [26], where the EFT approach is shown to result

from a valid ultraviolet (UV) model ; therefore, EFT is viable for vector-DM interpretations. The UV completion models have been investigated in two scenarios: along with the EFT approaches and in a separate model with additional fermions [27] .

This note is organized as follows: common notations used in the analyses are presented in Section 2.1. EFT approaches and UV complete models are described and discussed in Sections 2.2, 2.3, 2.4 and 2.5. In Section 3, we discuss the cases of vector dark matter (VDM)-nucleon interactions. Dark matter in the sub-GeV mass range is presented in Section 4. The note is summarized in Section 5.

2 Analysis

2.1 Common convention

Throughout the paper, the following conventions are utilized frequently:

1. H: 125 GeV Higgs boson.

2. $v = 246$ GeV: Higgs field's vacuum expectation value.

3. $m_\mathrm{N} = 0.938$ GeV: proton-nucleon mass.

4. m_V : vector boson mass.

5. $m_H = 125$ GeV: Higgs boson mass.

6. $\beta_V = \sqrt{1 - 4\frac{m_V^2}{m_H^2}}$

7. $\beta_\mathrm{VH} = \sqrt{1 - 4\frac{m_V^2}{m_H^2}\left(1 - 4\frac{m_V^2}{m_H^2} + 12\frac{m_V^4}{m_H^4}\right)}$

8. $\mu_{VN}^2 = \frac{m_V^2 m_N^2}{m_V^2 + m_N^2}$: vector DM reduced mass.

9. $\mathcal{B}_{H\rightarrow\mathrm{inv}}$: Branching ratio of $H \rightarrow$ invisible, upper limit at 90% CL of 11% is used as the result from the recently published VBF+MET analysis [28].

10. $\Gamma^{inv}(H \rightarrow VV) = \Gamma_\mathrm{inv}^\mathrm{H} = \mathcal{B}_{H\rightarrow\mathrm{inv}}\Gamma_H^{tot} = \frac{\mathcal{B}_{H\rightarrow\mathrm{inv}}}{1-\mathcal{B}_{H\rightarrow\mathrm{inv}}}\Gamma_H^{SM}$

11. $\Gamma_H^{SM} = 0.00407$ GeV: Higgs width at $m_H = 125$ GeV

12. $\hbar c = 1.97327\mathrm{e}^{-14}$ GeV $\times cm$

13. $f_N = 0.308(18)$: Higgs-nucleon form factor [29]

2.2 Effective Field Theory approach

In LHC Run–1 papers [23, 24] where $H \rightarrow$ invisible combination was done, the 90% CL upper limit on $\mathcal{B}_{H\rightarrow\mathrm{inv}}$ was converted into 90% CL upper limit on σ^SI(WIMP-N) with WIMP being either a scalar, a fermion or a vector boson by using the EFT approach [7]. In the scope of this note, only the VDM interpretation is discussed.

This approach suggests a model-independent Lagrangian for HVV coupling as the following (Equation 1 of Ref. [7]):

$$\mathcal{L}_V = \frac{1}{2}m_\mathrm{V}^2 V_\mu V^\mu + \frac{1}{4}\lambda_V(V_\mu V^\mu)^2 + \frac{\lambda_\mathrm{hVV}}{4}H^\dagger H V_\mu V^\mu. \tag{1}$$

The second term in Eq. 1 is for self–interaction and it is ignored; λ_V is the self interaction coupling for the vector. The Lagrangian has only two free parameters: HVV coupling λ_{hVV} and vector mass m_V. Using this Lagrangian, $\sigma^{SI}(V\text{-}N)$ together with Higgs invisible decay width Γ^H_{inv} are derived as functions of m_V and λ_{VH} as follow (Equations 4 and 5 of Ref. [7]):

$$\Gamma^{inv}(H \to VV) = \lambda_{HVV}^2 \frac{v^2 \beta_{VH} m_H^3}{512\pi m_V^4} \tag{2}$$

$$\sigma^{SI}(V\text{-}N)_{EFT} = \lambda_{HVV}^2 \frac{m_N^2 f_N^2}{16\pi m_H^4 (m_V + m_N)^2} \tag{3}$$

Extracting the coulping λ_{HVV} from Equation 2 and substitute into Equation 3, one can find a direct relation between $\sigma^{SI}(V\text{-}N)$ and Γ^H_{inv}:

$$\lambda_{HVV}^2 = \Gamma^{inv}(H \to VV) \frac{512\pi m_V^4}{v^2 \beta_{VH} m_H^3} \tag{4}$$

$$\sigma^{SI}(V\text{-}N)_{EFT} = \Gamma^{inv}(H \to VV) \frac{512\pi m_V^4}{v^2 \beta_{VH} m_H^3} \times \frac{m_N^2 f_N^2}{16\pi m_H^4 (m_V + m_N)^2}$$

$$\sigma^{SI}(V\text{-}N)_{EFT} = \Gamma^{inv}(H \to VV) \frac{32 m_V^4 m_N^2 f_N^2}{v^2 \beta_{VH} m_H^7 (m_V + m_N)^2}$$

$$\sigma^{SI}(V\text{-}N)_{EFT} = 32 \mu_{VN}^2 \Gamma^H_{inv} \frac{m_V^2 m_N^2 f_N^2}{v^2 \beta_{VH} m_H^7} \tag{5}$$

Using Equation 5 one can transform the limit on $\mathcal{B}_{H \to inv}$ into the vector line interpretation as in the green hashed band in Figure 9 of Ref. [23]. That figure shows the ATLAS Run–1 upper limit at the 90% CL on the WIMP–nucleon scattering cross section in a Higgs portal model as a function of the mass of the dark-matter particle, for a scalar, Majorana fermion, or vector-boson WIMP. LHC interpreted VDM limit in EFT was claimed to be model-independent and better than limits from direct detection in the regime of $m_V < \frac{m_H}{2}$. However, it drew controversial attention which will be discussed in Section 2.3.

2.3 Objection on EFT, first UV model

In the EFT approach used in LHC Run–1 [23], the mass of the VDM was entered arbitrarly, which leads to a non-renormalisable Lagrangian and violation of unitarity [25]. For this reason, it is safer to consider a better framework, i.e. a simple UV completion with a dark Higgs sector that gives mass to the vector DM via spontaneous electroweak symmetry breaking (EWSB). The simplest renormalisable Lagrangian for the Higgs portal VDM in such a UV model is given by Ref.[25]:

$$\mathcal{L}_{VDM} = -\frac{1}{4} V_{\mu\nu} V^{\mu\nu} + D_\mu \Phi^\dagger D^\mu \Phi - \lambda_\Phi (\Phi^\dagger \Phi - \frac{\nu_\Phi^2}{2})^2 - \lambda_{\Phi H}(\Phi^\dagger \Phi - \frac{\nu_\Phi^2}{2})(H^\dagger H - \frac{\nu_H^2}{2}), \tag{6}$$

where Φ is the dark Higgs field which generates a nonzero mass for the VDM through spontaneous $U(1)'$ breaking; $D_\mu \Phi = (\partial_u + i g_X Q_\Phi V_\mu)\Phi$ and g_X is the coupling constant.

From the Lagrangian, one can derive the invisible branching fraction of the Higgs decay [25]:

$$\Gamma^H_{inv} = \frac{g_X^2}{32\pi} \frac{m_H^3}{m_V^2} (1 - 4\frac{m_V^2}{m_H^2} + 12\frac{m_V^4}{m_H^4})(1 - 4\frac{m_V^2}{m_H^2})^{1/2}, \tag{7}$$

3

And then, the spin independent cross section of dark matter particles scattering, can be expressed as follows [25]:

$$\sigma^{\mathrm{SI}}(\text{V-N}) = cos^4(\theta)m_H^4 F(m_V, m_i, \nu) \times \sigma^{\mathrm{SI}}(\text{V-N})_{EFT}, \tag{8}$$

$$\simeq cos^4(\theta)(1 - \frac{m_H^2}{m_2^2}) \times \sigma^{\mathrm{SI}}(\text{V-N})_{EFT}, \tag{9}$$

Where θ is the mixing angle and m_2 is the mass of the dark Higgs boson. $\sigma^{\mathrm{SI}}(\text{V-N})_{EFT}$ is the spin independent cross section for vector DM particles from the EFT approach used in LHC Run–1 [23]. We can see that in the case of a UV completion model, the cross section has at least two additional parameters, the mass of the dark Higgs boson which is mostly singlet-like, and the mixing angle θ between the SM Higgs and the dark Higgs boson.
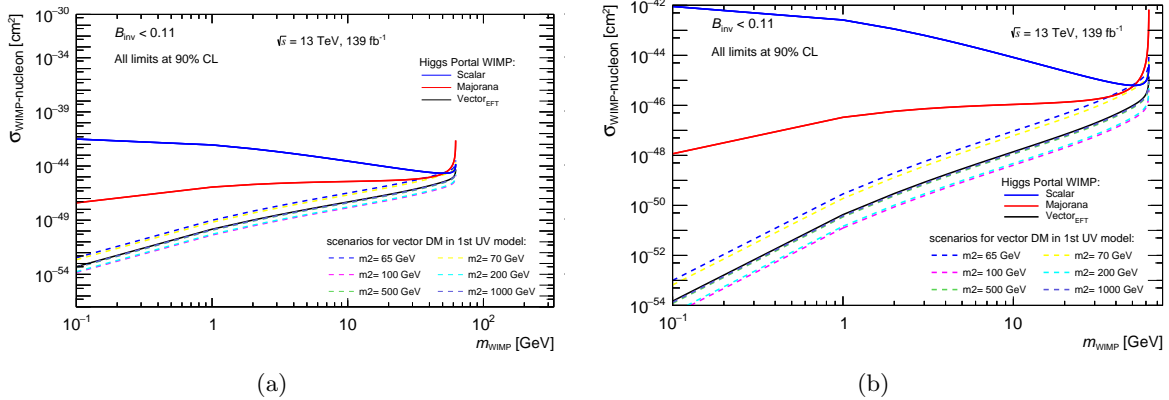

Figure 1: Spin independent cross section as function of the dark matter WIMP mass, displayed for Scalar, Majorana and vector Higgs portal models using EFT approach. The vector DM state case using the first UV model is shown in Figure 1(a), for the mixing angle $\theta = 0.2$, and for the dark Higgs mass: 65, 70, 100, 200, 500, 1000 GeV for dashed lines. A zoom around the vector EFT line is shown in Figure 1b to highlight the comparison between different scenarios of dark Higgs mass and the EFT approach.

We investigated how the cross section evolves for the choice of small mixing and for different scenarios of the dark Higgs mass m_2 in the range $[65, 1000]$ GeV(see Figure 1).

The resulting bound on $\sigma^{\mathrm{SI}}(\text{V-N})$ becomes weaker than the one based on EFT if the dark Higgs mass is lighter than the SM Higgs boson ($m_2 = 65, 70, 100$ GeV), and stronger if it is heavier than the SM Higgs boson ($m_2 = 200, 500, 1000$ GeV). In addtion, The UV model tends to coincide with EFT as the dark Higgs mass m_2 get larger (see Figure 1). The usual EFT approach applies only in the case of $m_2 = m_H cos(\theta)/\sqrt{1 + cos^2(\theta)}$ or $m_2 \to \infty$ and $\theta \to 0$. and therefore the bounds on the σ_p^{SI} should be taken with caution.

2.4 Reanalyse EFT, second UV model

In Ref.[26], theorists reanalyse the possibility that a Higgs-portal with a vectorial dark matter state could represent a consistent EFT of its UV completion. A dark Higgs sector was introduced to reproduce the vector mass via spontaneous electroweak symmetry breaking. Therefore the complete

Lagrangian for dark matter phenomenology is [26]:

$$\mathcal{L} = \frac{1}{2}\tilde{g}M_V(H_2 cos(\theta) - H sin(\theta))V_\mu V^\mu + \frac{1}{8}\tilde{g}^2(H^2 sin^2(\theta) - 2HH_2 sin(\theta)cos(\theta))$$
$$+ H_2^2 cos^2(\theta)V_\mu V^\mu, \qquad (10)$$

where H is the 125 GeV SM-like Higgs boson, H_2 is the dark Higgs boson and $\tilde{g}$ the new gauge coupling.

From the Lagrangian, one can derive the expression for Γ_{inv} and the spin independent cross section [26].

$$(\Gamma_{\text{inv}}^{\text{H}})_{U(1)} = \frac{\tilde{g}^2 sin^2(\theta)}{32\pi}\frac{m_H^3}{m_V^2}\beta_{VH}, \qquad (11)$$

$$\sigma^{\text{SI}}(\text{V-N}) = 32cos^2(\theta)\mu_{VN}^2\frac{m_V^2}{m_H^3}\frac{BR(H \to VV)\Gamma_H^{tot}}{\beta_{VH}} \times (\frac{1}{m_2^2} - \frac{1}{m_H^2})^2\frac{m_{N^2}}{v^2}|f_N^2|, \qquad (12)$$

Where β_{VH}, $BR(H \to VV) \equiv \Gamma(H \to VV)/\Gamma_H^{tot}$, μ_{V_p} are the same as in Section 2 and m_2 is the dark Higgs mass. The $\sigma^{\text{SI}}(\text{V-N})$ is different from the formula in Ref.[26]. The scale was corrected from 8 to 32 after discussions with the authors of Ref.[26]. The prediction for VDM using EFT approach can be obtained in the limit $cos^2(\theta)m_H^4(1/m_2^2 - 1/m_H^2)^2 \approx 1$ where $sin(\theta) << 1$ and $m_2 >> m_H$.

Similarly to the first UV model, We investigated the cross section for small mixing angles and various tuning values of the dark Higgs boson m_2 in the range $[65, 1000]$ GeV(see Figure 2).
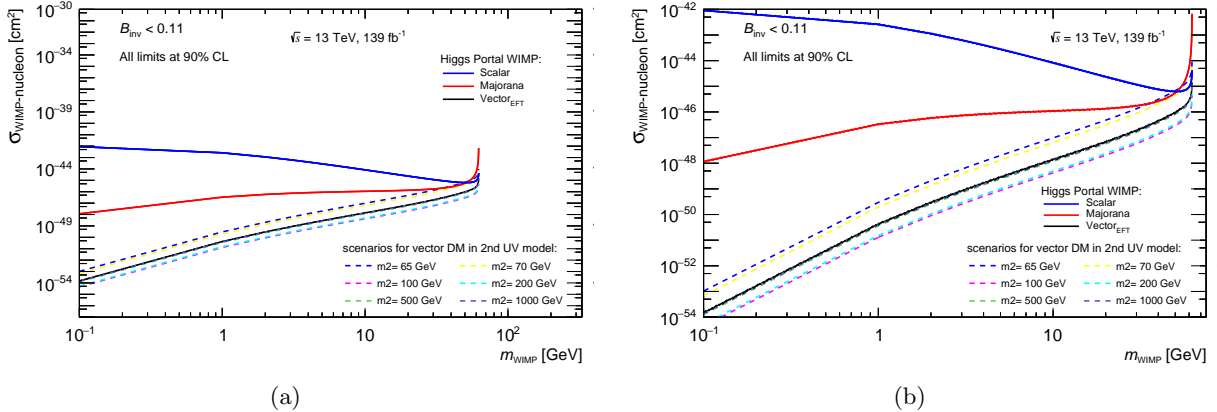

Figure 2: Spin independent cross section as function of the dark matter WIMP mass, displayed for Scalar, Majorana and vector Higgs portal models using EFT approach. The vector DM state case using the second UV model is shown in Figure 1(a), for the mixing angle $\theta = 0.2$, and for the dark Higgs mass: 65, 70, 100, 200, 500, 1000 GeV for dashed lines. A zoom around the vector EFT line is shown in Figure 1b to highlight the comparison between different scenarios of dark Higgs mass and the EFT approach.

This exercise is extremely important not only because it shows the difference between the EFT and its UV completion according to values of (θ, m_2), but also because it demonstrates that EFT approach could be a viable limit of the renormalisable model in a large region of its parameter space.

We have checked that the models introduced in Sections 2.3 and 2.4 are equivalent and agree when the parameters are chosen consistently.

2.5 Radiative Higgs portal, third UV model

2.5.1 Lagrangian

This UV model [27] uses the same approach as introduced in other UV models mentioned in Sections 2.3 and 2.4. The vector DM is introduced as a gauge field of a $U(1)'$ group which extends the SM symmetry; a Dark Higgs sector is added in to produce the vector boson mass via the Higgs spontaneous symmetry breaking mechanism. The Lagrangian of the vector part is as the following :

$$\mathcal{L} \supset -\frac{1}{4}V_{\mu\nu}V^{\mu\nu} + (D_\mu\Phi)^\dagger(D^\mu\Phi) - V(\Phi) + \lambda_P|H|^2|\Phi|^2 \tag{13}$$

where λ_P is the mixing parameter between the SM Higgs boson and the dark Higgs mode of the field Φ (Equation 2 of Ref. [27]). This model has a distinctive feature in generating the HVV coupling, and the fermions charged under SM×$U(1)'$ are added in, as shown below for the fermionic part of the Lagrangian :

$$\mathcal{L} \supset -m\epsilon^{ab}(\psi_{1a}\chi_{1b} + \psi_{2a}\chi_{2b}) - m_n n_1 n_2 - y_\psi\epsilon^{ab}(\psi_{1a}H_b n_1 + \psi_{2a}H_b n_2)$$
$$- y_\chi(\chi_1 H^* n_2 + \chi_2 H^* n_1) + h.c. \tag{14}$$

where ψ, χ, n are different fermion fields, a and b are $SU(2)_W$ indices, and H is the SM 125 GeV Higgs boson (Equation 4 of Ref. [27]). Fermions lead to loop induced HVV interaction as shown in Figure 3.
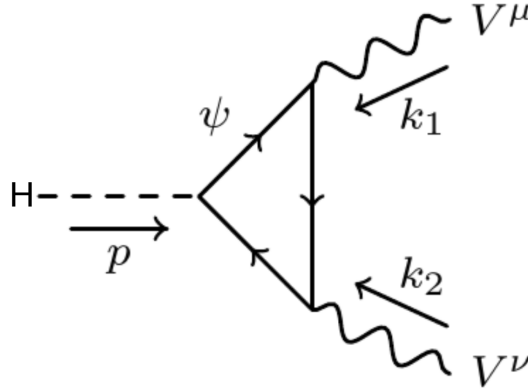

Figure 3: Fermion loop induced for HVV interaction. Figure 1 of Ref. [27]

2.5.2 Finding relation between σ^{SI}(V-N) and $\Gamma^{\text{H}}_{\text{inv}}$

There are many different scenarios for this UV model; the studied scenario in this note is the simplified case where the Higgs mixing parameter $\lambda_P \ll 1$, the charged fermions and the two heavier neutral states' masses are much heavier than the lightest neutral state mass, thus decouple from the Lagrangian. The minimal parameter space to be explored includes the vector mass m_{V}, the fermion mass m_{f}, the U(1)$'$ coupling g and the Yukawa coupling y of the added fermion to the SM Higgs.

This model has no direct analytical relation between $\Gamma^{\text{H}}_{\text{inv}}$ and σ^{SI}(V-N), and their computations are extensive. To obtain upper limit of σ^{SI}(V-N) versus m_{V} based on the upper limit on $\mathcal{B}_{H\to\text{inv}}$, one has to find values of (m_{f}, g, y) which satisfy the $\mathcal{B}_{H\to\text{inv}}$ upper limit within a certain precision, then calculate σ^{SI}(V-N). In our calculation, the $\mathcal{B}_{H\to\text{inv}}$ limit used is 11% at 90% CL from the recently published LHC analysis [28].

Explicitly, the task requires a scan through the set (m_f, g, y) for each m_V point to find values of Γ^H_{inv} corresponding to $\mathcal{B}_{H\to inv}$ of 11% [28] within a relative precision of 0.1-1.0%. The choice of 0.1-1.0% precision is arbitrary; they are shown to have negligible impact on the results. Therefore, the more stringent precision of 0.1% was considered. Some parts of the phase space can be left out of the scan since there are other constraints on those parameters:

- $m_V < \frac{m_H}{2}$, as for V being on-shell decay products of the Higgs boson.

- $m_f > \frac{m_H}{2}$, to forbid the SM Higgs to decay to the additional fermions.

- $0 < g, y < 4\pi$, as rule of thumb for dimensionless couplings satisfying perturbation.

- $0 < g^2 y < 40$, a model constraint [27].

All (m_f, g, y) sets that satisfy the corresponding 11% of the $\mathcal{B}_{H\to inv}$ are used to construct a band of σ^{SI}(V-N) versus m_V. Different coarse to fine scanning steps of 0.1 to 0.01 on (g, y) are performed while keeping the same step of 1 GeV for m_V and 5 GeV for m_f, as shown in Table 1.

Table 1: Scanning configurations for m_V and m_f, in context of the UV model in Ref. [27]

Variable	First bin	Last bin	Step
m_V (GeV)	1	62	1
m_f (GeV)	64	499	5

Coarse scan

Scanning steps of 0.1 on (g, y) are performed while keeping the same step of 1 GeV for m_V and 5 GeV for m_f as shown in Table 1. Detailed configurations for this scan can be found in Table 2. A relative precision of 0.1% on Γ^H_{inv} is required.

Table 2: Scanning configurations in the coarse scan for g and y in the context of UV model in Ref. [27].

Variable	First bin	Last bin	Step
g	0	12	0.1
y	0	12	0.1

Fine scan

Scanning steps of 0.01 on (g, y) are performed while keeping the same step of 1 GeV for m_V and 5 GeV for m_f as shown in Table 1. Detailed configurations for this scan can be found in Table 3. A relative precision of 1% on Γ^H_{inv} is required.

For both scans, all the found (m_f, g, y) for each m_V point are used to calculate σ^{SI}(V-N). The cross section values are then sorted from lowest to highest for each m_V point and plotted in Figure 4. Discussion about the plots is presented in the next section.

Table 3: Scanning configurations in the fine scan for g and y in the context of the UV model in Ref. [27].

Variable	First bin	Last bin	Step
g	0	12	0.01
y	0	12	0.01

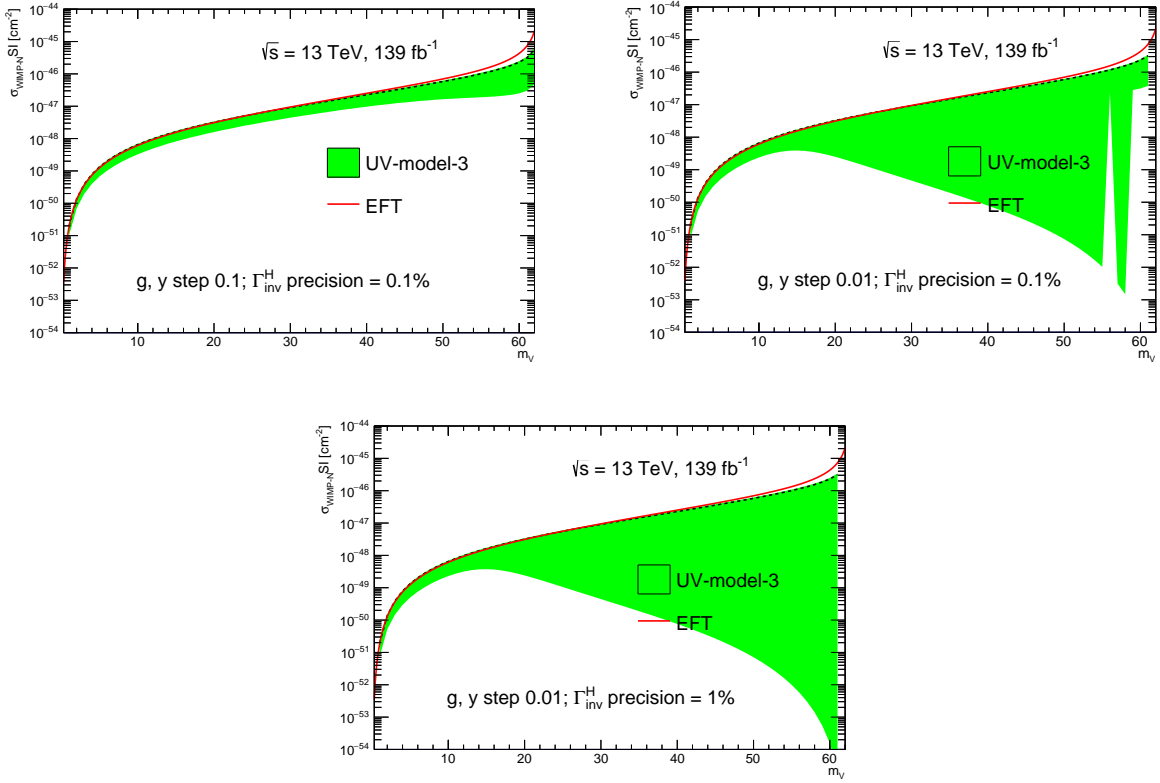
Figure 4: Green bands of upper limit on σ^{SI}(V-N) from coarse scan in Table 2 (upper left canvas), fine scan from Table 3 (upper right) and fine scan from Table 3 with looser precision of Γ^{H}_{inv} (down canvas) are shown in comparison with EFT red line, for the UV model in Ref. [27].

8

2.5.3 Results

Figures 4 and 5 show that the precision on $\Gamma_{\text{inv}}^{\text{H}}$ does not affect the upper bound on the $\sigma^{\text{SI}}(\text{V-N})$ as the dashed lines remain the same for all cases, and stay very close to the EFT limit. However, as seen in the second and third plots of Figure 4, the fine scanning of (g, y) extends the lower bound of the green bands meaning that going finer in (g, y) one can achieve much better limits on $\sigma^{\text{SI}}(\text{V-N})$ compared to EFT limit.
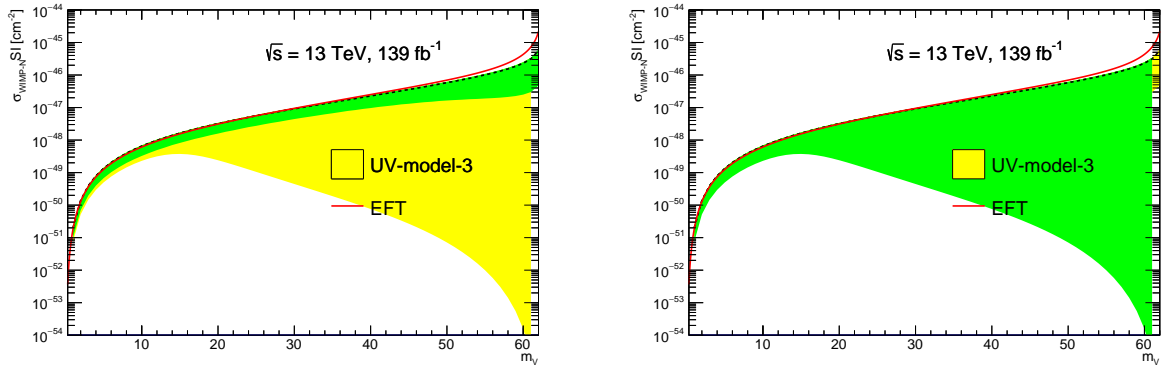

Figure 5: Superimposition of the interpretations for a coarse scan on top of a fine scan (left canvas) and vice versa (right canvas), for the UV model in Ref. [27].

3 Proposal

In this section we present our proposal of the Higgs portal VDM interpretation of the spin-independent dark-matter nucleon elastic scattering cross section using the invisible Higgs decay width. We propose to re-introduce the VDM limits in the LHC Higgs portal DM interpretation plots. This proposal is motivated by the results presented in Section 2 and could be split in three parts.

Firstly, The limitations of EFT approach as violation of unitarity and non-renormalisable Lagrangian (claimed in Section 2.3) is refuted by the recent review which derived the EFT Lagrangian from a certain UV model as shown in Section 2.4. This shows that the EFT approach is viable in the limit of a heavy additional scalar and small mixing angle.

Secondly, we propose to show the worst and best case scenarios of of the models described in Sections 2.3 and 2.4.

Thirdly, we propose to display the upper bound line of the UV-Model-3 discussed in Section 2.5, as shown with cyan in Figure 6.

Our full proposal is shown in Figure 6, where the interpretation of the radiative Higgs portal (third UV model) compared with EFT limit and with best and worst limit from the first UV model in m_2 range range of $[65, 1000]$ GeV. Also the most stringent limits currently available from direct detection experiments are shown for comparison [30–32]. The neutrino floor for coherent elastic neutrino-nucleus scattering of astrophysical neutrino is added in [33–35].
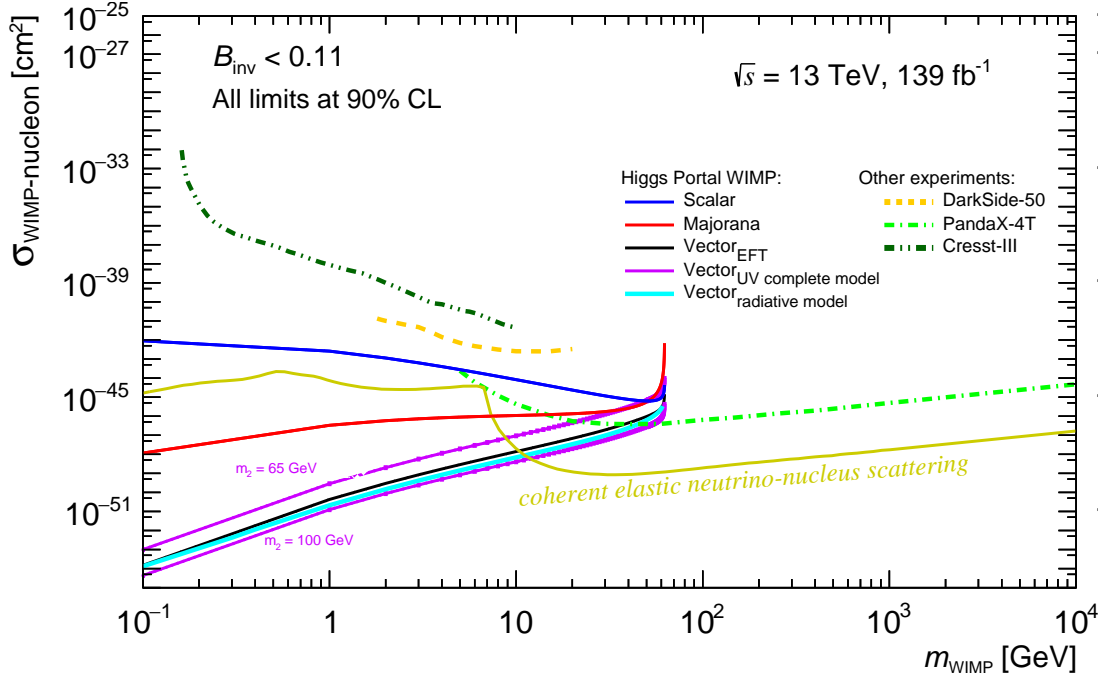
Figure 6: Upper limits on spin-independent WIMP-nucleon cross section using Higgs portal interpretations of B_{inv} at 90% CL as a function of the WIMP mass for scalar, majorana and vector states. For the vector hypothesis, the interpretation from EFT, UV complete and radiative models are presented respectively in black, magenta and cyan colours. Two scenarios are displayed for the UV complete model corresponding to the best and worst limits giving the mass of the dark Higgs in the range [65,1000] GeV. Results from direct detection experiments and the neutrino floor for coherent elastic neutrino-nucleus scattering are added for comparison [30–32, 35].

4   Extension to Sub-GeV WIMP masses

The LHC Higgs-portal DM interpretation of σ^{SI}(WIMP-N) has been so far shown for m_{V} ranging from 1 GeV to $\frac{m_H}{2}$. The upper edge at $\frac{m_H}{2}$ is for WIMP candidates to be produced on-shell from a Higgs decay. Whereas the lower edge at 1 GeV is arbitrarily coming from different considerations. The first consideration is about the theoretical or cosmological constraint on the WIMP mass. However, Particle Data Group 2019 review on DM shows the possibility of going to sub-GeV regime in many BSM models with WIMP paradigm [36]. Sections 26.6.2 and 26.6.3 of the PDG review discussed solid-state cryogenic detector experiment such as CRESST-III [30] which probes DM mass down to ~ 160 MeV.

LHC Dark Matter Working Group (LHCDMWG) white paper [37] has recommendations for interpretation of simplified DM models which have s-channel spin-1 mediators decaying to fermions (invisible, aka DM candidates). To predict the relic density, the LHCDMWG recommends to work under the assumption that the DM annihilation cross section of the predicted models is fully responsible for the DM number density [37]. That leads to Figures 3 and 4 of Ref. [37] to have DM mass lower bound at few GeV. However, the mentioned bench mark models do not include Higgs portal scenario in which the scalar Higgs boson is the mediator.

The second consideration is about the uncertainty on the σ^{SI}(WIMP-N) calculation via a Higgs mediator for LHC interpretation in the WIMP sub-GeV mass regime. That calculation depends on the coupling of the Higgs boson to a single nucleon, first calculated in Ref. [38] and further improved in Ref. [29] whose f_N value of 0.308(18) is then used in Refs. [28, 39]. These calculations use lattice QCD formalisms which are valid continuously from negative momentum transfer to positive momentum transfer, thus valid for 0-momentum transfer (our case of WIMP-nucleon elastic scattering). Interactions with the main author of Ref. [29] resolves the consideration about f_N vs sub-GeVmass.

In conclusion, the aforementioned considerations are not relevant to limit the LHC Higgs portal interpretations above 1 GeV. Therefore, we propose to show in the LHC Higgs portal interpretation plot, WIMP masses down to 0.1 GeV—as shown in Figure 2 of Ref. [26].

5   Conclusion

Several approaches for the interpretation of σ^{SI}(V-N) in Higgs-portal DM scenarios are presented. EFT approach is reviewed and shown to be safe to be reinserted in the LHC Higgs portal interpretation plot. Three UV models are studied, their results all are shown in different parameter phase spaces. In the first two UV models [25, 26], EFT is recovered when getting limits in certain region of their parameter phase spaces. Whereas for the third UV model [27], result in a simplified regime is better than the EFT approach limits. Therefore our final proposal for the LHC Higgs portal interpretation plot is to reinsert the EFT VDM line, include the upper bound of the third UV model, and the worst-best lines of the first and second UV models. Additionally, WIMP masses in the sub-GeV regime are discussed and proposed to be extended to 0.1 GeV in the LHC Higgs portal interpretation plot.

References

[1] D. Clowe et al., *A Direct Empirical Proof of the Existence of Dark Matter*, The Astrophysical Journal **648** (2006) L109, ISSN: 1538-4357, URL: http://dx.doi.org/10.1086/508162 (cit. on p. 1).

[2] J. L. Feng and J. Kumar, *The WIMPless Miracle: Dark-Matter Particles without Weak-Scale Masses or Weak Interactions*, Phys. Rev. Lett. **101** (2008) 231301, arXiv: 0803.4196 [hep-ph] (cit. on p. 1).

[3] I. Antoniadis, M. Tuckmantel, and F. Zwirner, *Phenomenology of a leptonic goldstino and invisible Higgs boson decays*, Nucl. Phys. **B707** (2005) 215, arXiv: hep-ph/0410165 [hep-ph] (cit. on p. 1).

[4] N. Arkani-Hamed, S. Dimopoulos, G. R. Dvali, and J. March-Russell, *Neutrino masses from large extra dimensions*, Phys. Rev. **D65** (2001) 024032, arXiv: hep-ph/9811448 [hep-ph] (cit. on p. 1).

[5] A. Datta, K. Huitu, J. Laamanen, and B. Mukhopadhyaya, *Invisible Higgs in theories of large extra dimensions*, Phys. Rev. **D70** (2004) 075003, arXiv: hep-ph/0404056 [hep-ph] (cit. on p. 1).

[6] S. Kanemura, S. Matsumoto, T. Nabeshima, and N. Okada, *Can WIMP Dark Matter overcome the Nightmare Scenario?*, Phys. Rev. **D82** (2010) 055026, arXiv: 1005.5651 [hep-ph] (cit. on p. 1).

[7] A. Djouadi, O. Lebedev, Y. Mambrini, and J. Quevillon, *Implications of LHC searches for Higgs–portal dark matter*, Phys. Lett. B **709** (2012) 65, arXiv: 1112.3299 [hep-ph] (cit. on pp. 1–3).

[8] A. Djouadi, A. Falkowski, Y. Mambrini, and J. Quevillon, *Direct Detection of Higgs-Portal Dark Matter at the LHC*, Eur. Phys. J. **C73** (2013) 2455, arXiv: 1205.3169 [hep-ph] (cit. on p. 1).

[9] R. E. Shrock and M. Suzuki, *Invisible decays of Higgs bosons*, Physics Letters B **110** (1982) 250, ISSN: 0370-2693, URL: http://www.sciencedirect.com/science/article/pii/0370269382912473 (cit. on p. 1).

[10] D. Choudhury and D. P. Roy, *Signatures of an invisibly decaying Higgs particle at LHC*, Phys. Lett. **B322** (1994) 368, arXiv: hep-ph/9312347 [hep-ph] (cit. on p. 1).

[11] O. J. P. Eboli and D. Zeppenfeld, *Observing an invisible Higgs boson*, Phys. Lett. **B495** (2000) 147, arXiv: hep-ph/0009158 [hep-ph] (cit. on p. 1).

[12] H. Davoudiasl, T. Han, and H. E. Logan, *Discovering an invisibly decaying Higgs at hadron colliders*, Phys. Rev. **D71** (2005) 115007, arXiv: hep-ph/0412269 [hep-ph] (cit. on p. 1).

[13] R. M. Godbole, M. Guchait, K. Mazumdar, S. Moretti, and D. P. Roy, *Search for 'invisible' Higgs signals at LHC via associated production with gauge bosons*, Phys. Lett. **B571** (2003) 184, arXiv: hep-ph/0304137 [hep-ph] (cit. on p. 1).

[14] D. Ghosh, R. Godbole, M. Guchait, K. Mohan, and D. Sengupta, *Looking for an Invisible Higgs Signal at the LHC*, Phys. Lett. **B725** (2013) 344, arXiv: 1211.7015 [hep-ph] (cit. on p. 1).

[15] G. Belanger, B. Dumont, U. Ellwanger, J. F. Gunion, and S. Kraml, *Status of invisible Higgs decays*, Phys. Lett. **B723** (2013) 340, arXiv: 1302.5694 [hep-ph] (cit. on p. 1).

[16] D. Curtin et al., *Exotic decays of the 125 GeV Higgs boson*, Phys. Rev. **D90** (2014) 075004, arXiv: 1312.4992 [hep-ph] (cit. on p. 1).

[17] F. Petricca et al., "First results on low-mass dark matter from the CRESST-III experiment", *15th International Conference on Topics in Astroparticle and Underground Physics (TAUP 2017) Sudbury, Ontario, Canada, July 24-28, 2017*, 2017, arXiv: 1711.07692 [astro-ph.CO] (cit. on p. 1).

[18] E. Behnke et al., *Final Results of the PICASSO Dark Matter Search Experiment*, Astropart. Phys. **90** (2017) 85, arXiv: 1611.01499 [hep-ex] (cit. on p. 1).

[19] D. S. Akerib et al., *Results from a search for dark matter in the complete LUX exposure*, Phys. Rev. Lett. **118** (2017) 021303, arXiv: 1608.07648 [astro-ph.CO] (cit. on p. 1).

[20] X. Cui et al., *Dark Matter Results From 54-Ton-Day Exposure of PandaX-II Experiment*, Phys. Rev. Lett. **119** (2017) 181302, arXiv: 1708.06917 [astro-ph.CO] (cit. on p. 1).

[21] E. Aprile et al., *Dark Matter Search Results from a One Ton-Year Exposure of XENON1T*, Phys. Rev. Lett. **121** (2018) 111302, arXiv: 1805.12562 [astro-ph.CO] (cit. on p. 1).

[22] P. Agnes et al., *Low-Mass Dark Matter Search with the DarkSide-50 Experiment*, Phys. Rev. Lett. **121** (2018) 081307, arXiv: 1802.06994 [astro-ph.HE] (cit. on p. 1).

[23] G. Aad et al., *Constraints on new phenomena via Higgs boson couplings and invisible decays with the ATLAS detector*, JHEP **11** (2015) 206, arXiv: 1509.00672 [hep-ex] (cit. on pp. 1–4).

[24] P. Calfayan, *Searches for invisible Higgs boson decays with ATLAS and CMS*, tech. rep., CERN, 2015, URL: https://cds.cern.ch/record/2058131 (cit. on pp. 1, 2).

[25] S. Baek, P. Ko, and W.-I. Park, *Invisible Higgs decay width vs. dark matter direct detection cross section in Higgs portal dark matter models*, Physics Letters B (2014), ISSN: 0370-2693, URL: http://www.sciencedirect.com/science/article/pii/S0370269314006984 (cit. on pp. 1, 3, 4, 11).

[26] G. Arcadi, A. Djouadi, and M. Kado, *The Higgs-portal for vector Dark Matter and the Effective Field Theory approach: a reappraisal*, Phys. Lett. B **805** (2020) 135427, arXiv: 2001.10750 [hep-ph] (cit. on pp. 1, 4, 5, 11).

[27] A. DiFranzo, P. J. Fox, and T. M. P. Tait, *Vector Dark Matter through a Radiative Higgs Portal*, JHEP **04** (2016) 135, arXiv: 1512.06853 [hep-ph] (cit. on pp. 2, 6–9, 11).

[28] *Search for invisible Higgs boson decays with vector boson fusion signatures with the ATLAS detector using an integrated luminosity of 139 fb^{-1}*, tech. rep. ATLAS-CONF-2020-008, CERN, 2020, URL: http://cds.cern.ch/record/2715447 (cit. on pp. 2, 6, 7, 11).

[29] M. Hoferichter, P. Klos, J. Menéndez, and A. Schwenk, *Improved limits for Higgs-portal dark matter from LHC searches*, Phys. Rev. Lett. **119** (2017) 181803, arXiv: 1708.02245 [hep-ph] (cit. on pp. 2, 11).

[30] A. Abdelhameed et al., *First results from the CRESST-III low-mass dark matter program*, Phys. Rev. D **100** (2019) 102002, arXiv: 1904.00498 [astro-ph.CO] (cit. on pp. 9–11).

[31] A. et all, *Low-Mass Dark Matter Search with the DarkSide-50 Experiment*, Physical Review Letters **121** (2018), ISSN: 1079-7114, URL: http://dx.doi.org/10.1103/PhysRevLett.121.081307 (cit. on pp. 9, 10).

[32] Y. M. et all, *Dark Matter Search Results from the PandaX-4T Commissioning Run*, 2021, arXiv: 2107.13438 [hep-ex] (cit. on pp. 9, 10).

[33] J. Billard, E. Figueroa-Feliciano, and L. Strigari, *Implication of neutrino backgrounds on the reach of next generation dark matter direct detection experiments*, Physical Review D **89** (2014), ISSN: 1550-2368, URL: http://dx.doi.org/10.1103/PhysRevD.89.023524 (cit. on p. 9).

[34] F. Ruppin, J. Billard, E. Figueroa-Feliciano, and L. Strigari, *Complementarity of dark matter detectors in light of the neutrino background*, Physical Review D **90** (2014), ISSN: 1550-2368, URL: http://dx.doi.org/10.1103/PhysRevD.90.083510 (cit. on p. 9).

[35] J. Billard, "Searching for Dark Matter and New Physics in the Neutrino sector with Cryogenic detectors", Habilitation à diriger des recherches: Université Claude Bernard Lyon 1, 2021, URL: https://tel.archives-ouvertes.fr/tel-03259707 (cit. on pp. 9, 10).

[36] 2. PdG, *M. Tanabashi et al. (Particle Data Group), Phys. Rev. D 98, 030001 (2018) and 2019 update.*, tech. rep., 2019, URL: https://pdg.lbl.gov/2019/reviews/rpp2019-rev-dark-matter.pdf (cit. on p. 11).

[37] A. Albert et al., *Recommendations of the LHC Dark Matter Working Group: Comparing LHC searches for dark matter mediators in visible and invisible decay channels and calculations of the thermal relic density*, Physics of the Dark Universe **26** (2019) 100377, ISSN: 2212-6864, URL: http://www.sciencedirect.com/science/article/pii/S2212686419301682 (cit. on p. 11).

[38] M. Shifman, A. Vainshtein, and V. Zakharov, *Remarks on Higgs-boson interactions with nucleons*, Physics Letters B **78** (1978) 443, ISSN: 0370-2693, URL: http://www.sciencedirect.com/science/article/pii/0370269378904811 (cit. on p. 11).

[39] ATLAS Collaboration, *Combination of searches for invisible Higgs boson decays with the ATLAS experiment*, Phys. Rev. Lett. **122** (2019) 231801, arXiv: 1904.05105 [hep-ex] (cit. on p. 11).